Article

A Bioorthogonal Small Molecule Selective Polymeric "Clickase"

Junfeng Chen, Ke Li, Sarah Bonson, and Steven C. Zimmerman

J. Am. Chem. Soc., **Just Accepted Manuscript** • DOI: 10.1021/jacs.0c06553 • Publication Date (Web): 14 Jul 2020

A Bioorthogonal Small Molecule Selective Polymeric "Clickase"

Junfeng Chen, Ke Li, Sarah E. Bonson, and Steven C. Zimmerman*

Supporting Information

ABSTRACT: Synthetic polymer scaffolds may serve as gatekeepers preventing the adhesion of biomacromolecules. Herein, we use gating to develop a copper-containing single-chain nanoparticle (SCNP) catalyst as an artificial "clickase" that operates selectively on small molecules that are able to penetrate the polymeric shell. Whereas the analogous clickase with surface ammonium groups performs highly efficient copper(I)-catalyzed alkyne–azide cyclo-addition (CuAAC) reactions on both alkynylated proteins and small molecule substrates, the new SCNP clickase with polyethylene glycol (PEG) groups is only active on small molecules. Further, the new SCNP resists uptake by cells allowing extracellular click chemistry to be performed. We describe two proof of principle applications that illustrate the utility of the bioorthogonal activity. First, the SCNP catalyst is able to screen for ligands that bind proteins, including proteolysis targeting chimera (PROTAC)-like molecules. Second, the non-membrane permeable SCNP can efficiently catalyze the click reaction extracellularly, thereby enabling in situ anticancer drug synthesis and screening without the catalyst perturbing intracellular functions.

INTRODUCTION

Gating has emerged as a useful strategy to control all aspects of chemical catalysis. By caging in a shell (Scheme 1), increased catalyst stability can be achieved and desired substrate selectivity controlled as the surrounding scaffold determines the molecules able to diffuse or bind to the catalytic center. The overall approach has been widely used in multiple areas of chemistry. For example, in supramolecular chemistry, cucurbituril has served as the gate-keeper of a nano-reactor[1] or a metal complex,[2] in both cases turning on and off catalysis by reversibly blocking access to the active site. Synthetic organic chemists have used metal-organic cages to encapsulate catalysts and alter their stability and accessibility.[3,4] An example in the biomaterials area involves a PEGylated polymeric micelle that was reported to protect an enzyme from antibody binding and protease degradation, while preserving its activity toward small molecule substrates.[5]

This work is focused on a type of gating by catalytic single-chain nanoparticles (SCNP). Catalytic SCNP have received considerable attention recent years.[6-12] The polymeric scaffold encapsulates and solubilizes the synthetic catalyst in water,[13,14] and binds substrates in proximity to the catalytic sites in an enzyme-like manner to achieve high efficiency.[15,16] Some cationic SCNPs are taken up by cells, retaining their activity and performing intracellular catalysis.[17,18] Neutral Jeffamine functionalized SCNP catalysts have also shown to be able to perform reactions in cells.[19] Previously, we reported the development of a copper containing SCNP as a "clickase." The water-soluble polyacrylamide SCNP**1** was covalently cross-linked with BTTAA-like ligands that are particularly effective at stabilizing Cu^{I}. The artificial clickase performed CuAAC reactions at unprecedented rates by binding small molecule substrates in interior pockets, which was referred to as "uptake mode."[20] Surprisingly we discovered that the same clickase performed highly efficient reactions on protein surfaces. Mechanistic studies showed that the macromolecule to biomacromolecule catalysis was realized through an "attach mode," wherein the SCNP supramolecularly attaches to the protein surface using multivalent interactions.

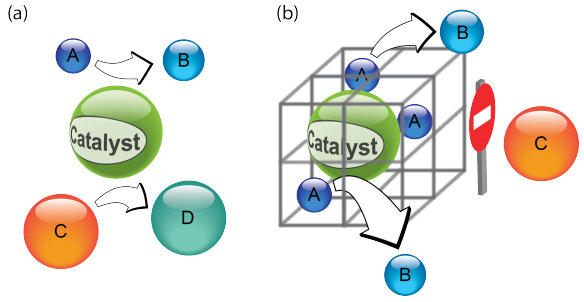

Scheme 1. Schematic illustration of catalyst (a) free in solution and (b) gated by encapsulation.

Given that the CuAAC reaction is one of the most widely used conjugation tools for organic chemistry and chemical biology,[21] we sought to expand the utility of Cu^{I}–SCNP**1** as a clickase. In particular, we sought an analogous SCNP that would retain the high CuAAC activity at micromolar concentrations of small molecule substrates in aqueous buffer,[22] but be fully bioorthogonal. Beyond the ability to bind proteins, Cu^{I}–SCNP**1** is taken up by cells through endocytosis, likely because the polycationic SCNP adheres to cell surfaces. Herein, we report Cu^{I}–SCNP**2** with surface PEG groups for water-solubility. This new catalyst performs the bioorthogonal CuAAC click reaction on small molecules with high efficiency, and exhibits its own bioorthogonality. Thus, Cu^{I}-SCNP**2** interacts with proteins weakly and is not taken up by cells, allowing proof of principle experiments such as in situ anticancer drug synthesis and screening for ligand-protein binding.

RESULTS AND DISCUSSION

Design and synthesis. SCNP**2** was prepared following our reported "folding and cross-linking" strategy.[20] Thus, poly(pentafluorophenyl acrylate) was post-functionalized with 6-aminohexanoic acid, 3-azidopropylamine, and the mono-$MePEG_{1000}$ amide of 1,10-decane diamine. The resulting azido polymer was intramolecularly cross-linked with *N,N*-dipropargyl-(1-(*tert*-butyl)-1*H*-1,2,3-triazol-4-yl)methanamine in water using the CuAAC reaction. The resulting covalent cross-linking groups are *N*-*tert*-butyl-tris(triazolyl)methylamine ligands that, together with the carboxylate groups, act analogously to BTTAA-like ligands.[23]

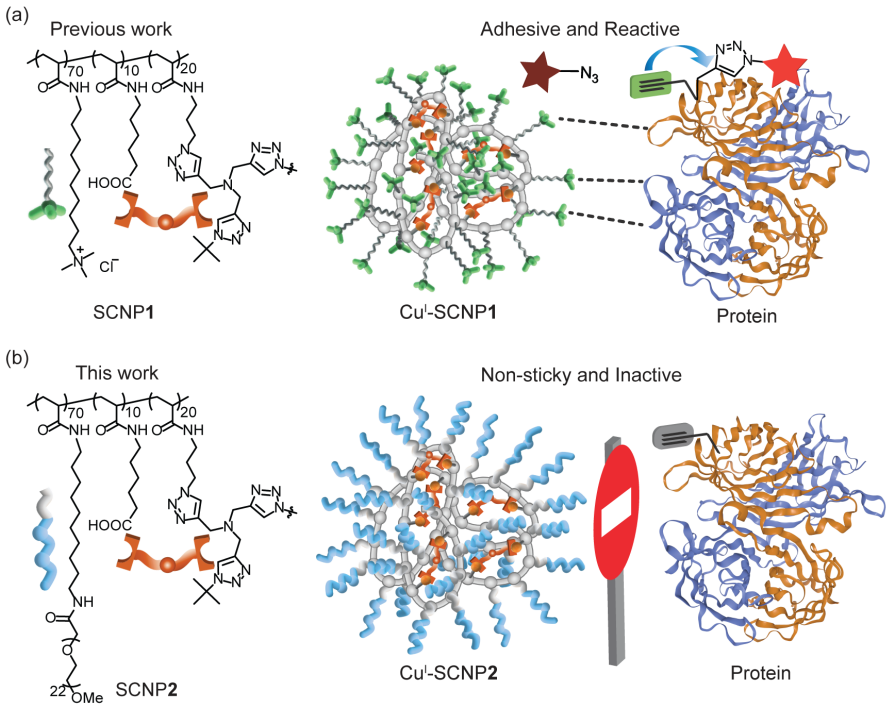

Figure 1. Schematic illustration of the two SCNP catalysts. (a) The structure of cationic SCNP**1** which binds and catalyzes reactions on protein surfaces. (b) The structure of PEGylated SCNP**2** which does not bind proteins and only perform reactions on small molecules.

The decyl linker units were chosen to provide a hydrophobic binding capacity analogous to that found in SCNP**1** whereas the PEG shell conferred water-solubility and resistance to protein and cell binding.

The nanoparticle was purified by dialyzing against water and characterized by dynamic light scattering (DLS, Figure 2a) and transmission electron microscopy (TEM, Figure S1). The diameter of SCNP**2** was found to be around 11 nm by DLS, which is higher than that for SCNP**1** (6-7 nm) due to its larger molecular weight. After the nanoparticle synthesis and purification, sufficient $CuSO_4$ was added to give a 1:1 ratio of copper ion to the tris-triazolylmethylamine crosslinks to give Cu^{II}–SCNP**2**, which can be reduced by sodium ascorbate (NaAsc) to generate the catalytically active Cu^{I}–SCNP**2** in situ.

SCNP-protein binding study. Replacing the cationic trimethylammonium ion groups with PEG groups gives SCNP**2** with a potentially uncharged neutral surface, depending on the location and ionization of the carboxylic acid groups. Indeed, the measured ζ-potential for SCNP**1** and SCNP**2** were 33.9 ± 1.7 mV and 1.57 ± 0.64 mV, respectively (Figure 2a), indicating a nearly neutral surface for the latter polymeric nanoparticle. Previously, we reported that the carboxylate groups in SCNP**1** accelerated its click reaction analogous to that found in the small molecule ligand BTTAA.[23] The low ζ-potential for SCNP**2** may indicate that the carboxylic acid groups are protonated, form zwitterionic structures with the tertiary amino groups, or, more likely that the PEG groups provide a neutral surface layer.

To assess its adhesive character, bovine serum albumin (BSA) was chosen as the model protein to measure the potential for SCNP binding. The interaction between BSA with Cu^{II}–SCNP**1** or Cu^{II}–SCNP**2** was measured by using STD spectroscopy,[24] which uses the nuclear Overhauser effect (NOE) to assess the nature of possible intermolecular interactions. The nanoparticles were mixed with BSA in 1:1 molar ratio in deuterated PBS buffer, and the STD spectra were acquired by irradiating the mixture at 7.0 ppm, the protein aromatic region. The STD signals corresponding to the trimethyl ammonium on SCNP**1**, the PEG groups on SCNP**2** and the hydrophobic alkyl chains for both SCNPs were measured and the % STD calculated. As shown in Fig. 2b, the PEG and hexamethylene groups on SCNP**2** showed negligible and weaker STD signals, respectively with BSA. The magnitude of these differences is significant and consistent with weaker interactions.[25,26]

To further examine the potential interaction with proteins, a fluorescence anisotropy experiment was performed using fluorescein labeled BSA. As seen in Fig. 2c, SCNP**2** exhibited significantly lower polarization values than SCNP**1**. To assess the significance of this difference, the polarization of the SCNP**1**·BSA complex was reexamined with increasing sodium chloride concentration to lower the electrostatic binding (Figure S4). The reduced polarization is similar to that see in SCNP**2** and supports the reduced adhesion afforded by the PEG shell.

Protein vs. small molecule CuAAC activity. To test whether the PEG shell in SCNP**2** with its lower protein association translates into reduced uptake or attach mode catalysis, the rates of the CuAAC click reaction between Al**1** and alkynylated BSA (BSA-Al) were measured. BSA-Al was prepared by reacting BSA with the NHS-ester of 4-pentynoic acid, the protein product containing on average 13 alkyne groups as indicated by MALDI-MS.[20] To monitor the reactions at low concentration, a fluorogenic azido coumarin (Az**1**) was used as the azide substrate. Thus, Az**1** exhibits a large increase in fluorescence after the click reaction.[27] Fluorogenic reactions were performed in PBS buffer containing Az**1** (20 μM) with Al**1** (40 μM) or BSA-Al (2 μM) by using either Cu^{I}–SCNP**1** (2 μM) or Cu^{I}–SCNP**2** (2 μM). For reference, one of the fastest known small molecule catalysts Cu^{I}–BTTAA (20 μM) was used at the same copper concentration.[23]

Cu^{I}–SCNP**1** and Cu^{I}–SCNP**2** both showed high efficiency in catalyzing the click reaction between the small molecules Az**1** and

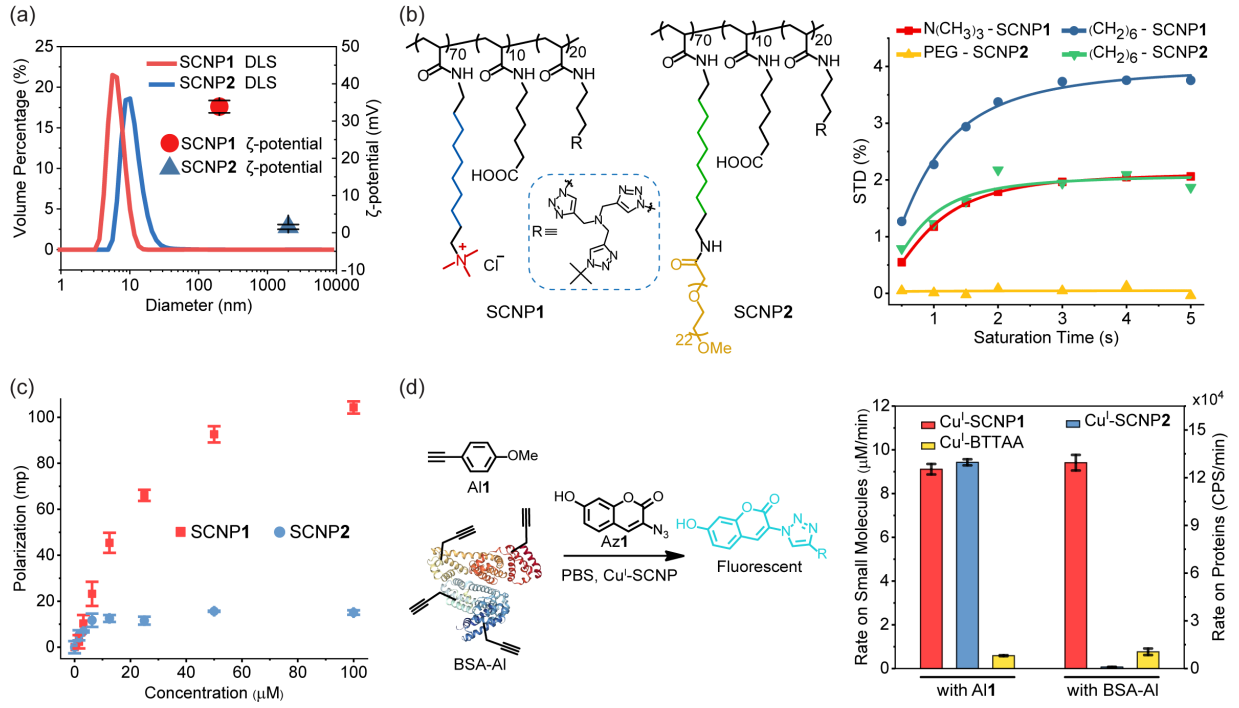

Figure 2. (a) DLS and ζ-potential data of SCNP**1** and SCNP**2**. (b) STD signal intensities of the trimethyl ammonium groups and alkyl chains on 100 μM Cu^{II}–SCNP**1** or Cu^{II}–SCNP**2** with 100 μM BSA in deuterated PBS buffer (1x, pD = 7.4) irradiated at 7.0 ppm. Trimethyl ammonium group and hydrophobic chains labelled with colors used in STD plot. (c) Fluorescence polarization of fluorescein labelled BSA (2 μM) with different concentration of Cu^{II}–SCNP**1** or Cu^{II}–SCNP**2** in PBS buffer (1x, pH = 7.4). (d) Initial reaction rates for small molecule and protein substrates with Cu^{II}–SCNP**1** (2 μM) or Cu^{II}–SCNP**2** (2 μM) in PBS buffer (1x, pH = 7.4) at room temperature. For small molecule substrate: Al**1** (40 μM) and Az**1** (20 μM). For protein substrate: BSA-Al (2 μM) and Az**1** (40 μM). Error bars represent the standard deviation of three independent experiments. Data for SCNP**1** and BTTAA from ref. 20.

Al**1**. Thus, both nanoparticles achieved >90% conversion within 5 min (Figure S2a), and their initial rates were around 15 times faster than that of Cu^{I}–BTTAA (Figure 2d).[23] As previously observed, Cu^{I}–SCNP**1** exhibited a high rate of reaction in protein labeling, performing the click reaction between BSA-Al and Az**1** 12-fold faster than Cu^{I}–BTTAA. However, Cu^{I}–SCNP**2** failed to catalyze the reactions on BSA-Al, exhibiting an 11 and 137-fold slower rate than that of Cu^{I}–BTTAA or Cu^{I}-SCNP**1**, respectively. The fluorogenic reactions were also performed on a mixture of Al**1** and BSA-Al, and Cu^{I}–SCNP**2** showed a 60-fold preference for the small molecule over the protein (Figure S2b). These results suggest that the PEG groups on the clickase block its active sites for protein substrates, while maintaining the capability to uptake and catalyze click reactions with small molecule substrates.

Protein-ligand binding study. Uptake mode catalysis by Cu^{I}–SCNP requires the nanoparticle to bind small molecules within their interior, the binding constants estimated to be in the micro-molar range.[16,20] If a protein binds a small molecule azide or alkyne with a comparable or lower K_D, its uptake mode click reaction would be inhibited, but only if attach mode is not operative (Figure 3a). The demonstration that the PEG groups in Cu^{I}–SCNP**1** prevent its interaction with proteins raises the interesting possibility that the nanoparticle might be used to screen for small molecules that are bound to proteins of interest. To test this hypothesis, fluorogenic reactions were performed between Az**1** and seven alkyne substrates with or without adding carbonic anhydrase II.

Carbonic anhydrase II (CA) was chosen as an inexpensive, readily available, and prevalent enzyme. Its inhibitors were once commonly used therapeutic agents, but now are limited mostly to glaucoma treatment. The proof of principle screen for CA binders used a reactivity index to estimate the small molecule binding capability. The reactivity index is defined as the ratio of the initial

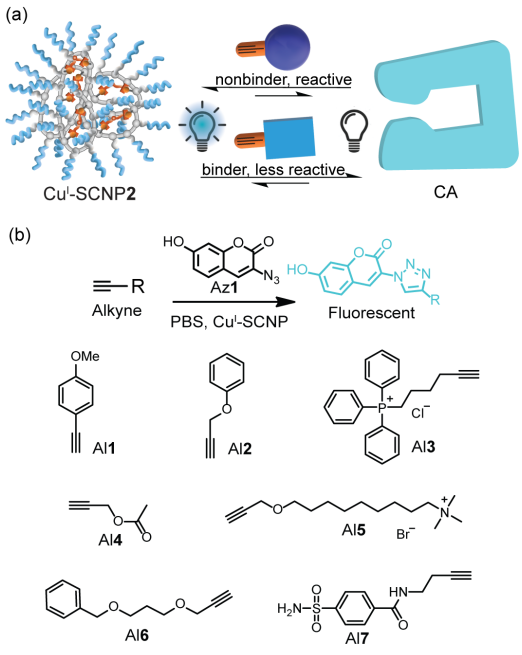

	Al1	Al2	Al3	Al4	Al5	Al6	Al7
Reactivity Index	0.87	0.95	0.88	0.99	0.92	1.06	**0.46**

Figure 3. Protein-ligand binding study by using Cu^{I}-SCNP**2**. (a) Illustration of competitive binding with proteins making nanoparticle only active on free substrates. (b) Chemical structure of alkyne substrates and their reactivity index. Fluorogenic reactions in PBS buffer: [Cu^{I}-SCNP**2**] = 4 μM, [Az**1**] = 2 μM, [NaAsc] = 200 μM and [Al] = 1 μM with/without [CA] = 2 μM.

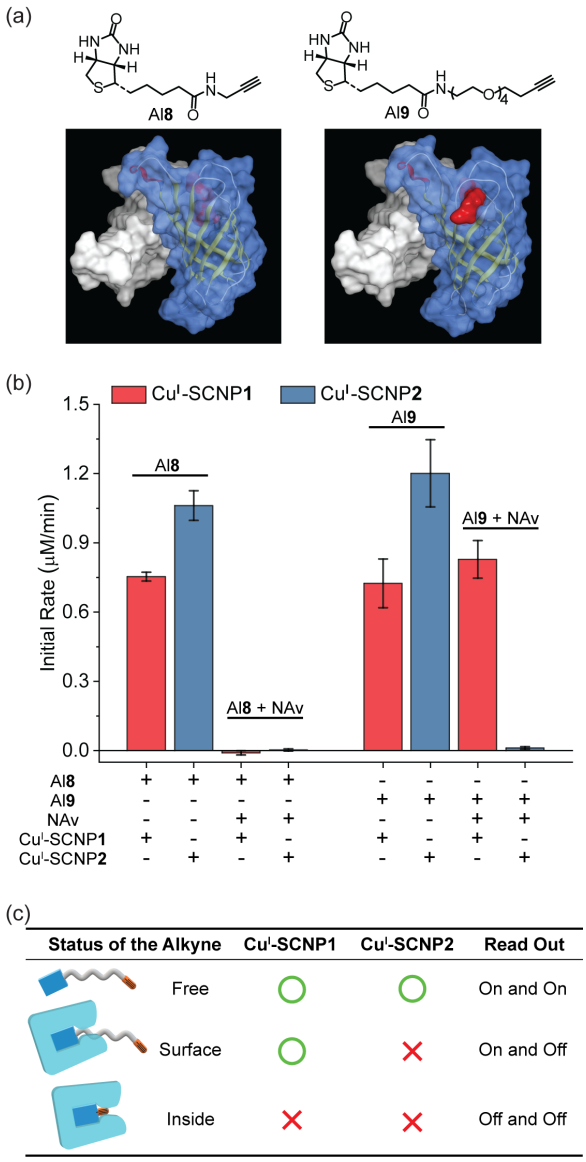

Figure 4. Activity of Cu^{I}-SCNP**1** and Cu^{I}-SCNP**2** on biotin-NAv complexes. (a) The chemical structures of two alkyne functionalized biotin compounds and the MOE simulation results of NAv-Al**8** and NAv-Al**9** complexes. (b) The initial reaction rates of fluorogenic reactions conducted in PBS buffer containing: [Cu^{I}-SCNP] = 4 μM, [Az**1**] = 2 μM, [NaAsc] = 200 μM and [Al] = 1 μM with/without [CA] = 2 μM. The error bars represent the standard deviation of three independent experiments. (c) Schematic illustration of the SCNP mediated fluorogenic protein-ligand binding assay.

rate of the click reaction with CA to that without CA. If an alkyne substrate binds to CA, it would become less accessible to Cu^{I}-SCNP**2**, producing a reactivity index lower than 1. If there is no interaction between the substrate and protein, the index should remain around 1, because the small molecule is free in solution to be taken up into the nanoparticle interior for the click reaction. As shown in Figure 3b, Al**1**-**6** exhibited reactivity index closed to 1, indicating they were nonbinding or weakly bound to CA. Al**7** was used because sulfamoyl compounds are known CA inhibitors.[28] Indeed, its reactivity index was significantly lower.

The activity of Cu^{I}–SCNP**1** and Cu^{I}–SCNP**2** toward protein-ligand complexes was studied in more detail. Thus, two biotin-alkyne derivatives that bind to neutravidin (NAv) tightly were prepared with either a short (Al**8**) or a long linker (Al**9**) (Figure 4a). NAv is the deglycosylated form of avidin and exhibits a neutral surface charge. The crystal structure of the Nav-biotin complex was obtained from the protein data bank (PDB, ID: 2AVI) and imported into the molecular operating environment (MOE) software. The biotin structure in the protein was mutated into Al**8** or Al**9** using the build feature in MOE, and the structure underwent energy minimization. Shown in Figure 4a are two identical subunits of NAv, one colored blue and the ligands colored red. For the NAv-Al**8** complex, the whole Al**8** substrate was buried inside the protein, whereas in NAv-Al**9**, the linker chain reaches out to the protein surface allowing the alkyne group to be accessed.

The initial rates of the CuAAC click reaction between Az**1** and either free ligands Al**8** and Al**9** or bound ligands NAv-Al**8** or NAv-Al**9** catalyzed by Cu^{I}-SCNP**1** and Cu^{I}-SCNP**2** were measured. As shown in Figure 4b, both nanoparticles behaved similarly with free and bound Al**8**. Thus, free ligand Al**8** reacts in uptake mode, but the neutravidin-bound Al**8** is inaccessible. Even with the longer linker group in NAv-Al**9**, Cu^{I}-SCNP**2** showed almost no activity in the click reaction with Az**1**, consistent with the observation that only free small molecules are reactive toward the PEGylated nanoparticle. These results indicate that protein-ligand binding can be assessed by using the two nanoparticles as the dual logical gates. As shown in Figure 4c, the assay would be conducted by performing fluorogenic reactions with Cu^{I}-SCNP**1** and Cu^{I}-SCNP**2** separately. The protein ligand interactions can be assessed via the fluorescence readout with three possibilities: free (on and on), on the protein surface and accessible (on and off) or bound to the protein interior and inaccessible (off and off).

Recently, proteolysis targeting chimera (PROTAC) technology has received considerable attention because of its potential to degrade pathogenic proteins and particularly to treat diseases originating from "undruggable" proteins, those for which a traditional inhibitor strategy is not available.[29] PROTAC ligands typically contain two different protein binding groups on each end of a linker, and thus are able to bring together the target protein and the protein degradation machinery. However, PROTAC binding is highly dependent on the environment and concentrations, and some suffer from the "hook effect," resulting in poor conjugation of the two proteins.[30] Thus, evaluating the binding status of both end-group ligands is essential in developing PROTAC ligands.

A PROTAC-inspired model compound, Al**10**, was synthesized with a biotin ligand and a sulfamoyl group for targeting for NAv and CA, respectively as well as an alkyne group adjacent to each binding moiety. In the absence of proteins, both Cu^{I}-SCNP**1** and Cu^{I}-SCNP**2** catalyzed the click reaction between Al**10** and Az**1** as was observed by a fluorescence increase (on and on). Upon adding NAv, Cu^{I}-SCNP**1** remained active exhibiting a reactivity index of ca. 1.2, whereas Cu^{I}-SCNP**2** showed almost no activity (Figure 5). This on and off fluorescence readout suggests that Al**10** was bound to NAv, most likely with the alkyne group next to the biotin group buried inside the protein scaffold and the other alkyne group exposed on the surface. When both NAv and CA were added to Al**10**, Cu^{I}-SCNP**2** remained inactive, whereas the initial rate of Cu^{I}-SCNP**1** decreased only ca. 20% (off and mostly on), indicating that the alkyne group on the sulfamoyl side remained partly available to Cu^{I}-SCNP**1**. This observation suggests that in the presence of both proteins there is an equilibrium mixture of CA-Al**10**-NAv and Al**10**-NAv. Overall, this model experiment demonstrates the potential use of Cu^{I}-SCNP**1** and Cu^{I}-SCNP**2** in a combination fluorogenic assay to test potential PROTAC ligands.

Cu^{I}-SCNP2 mediated extracellular synthesis and drug screening. Given the weak protein absorption, we wondered whether SCNP**2**,

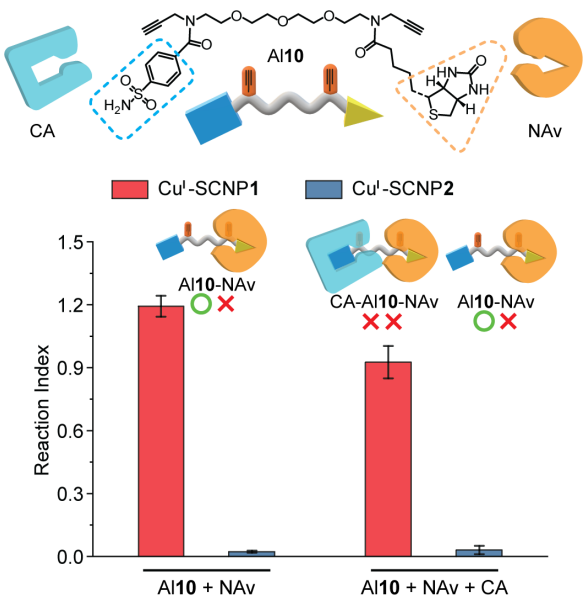

Figure 5. The chemical structure of Al**10** and the illustration of its binding towards CA and NAv. The initial reaction rates of fluorogenic reactions conducted in PBS buffer containing: [Cu^{I}-SCNP**2**] or [Cu^{I}-SCNP**2**] = 4 μM, [Az**1**] = 2 μM, [NaAsc] = 200 μM and [Al] = 1 μM with/without [NAv] = 0.4 μM or [CA] = 2 μM. The error bars represent the standard deviation of six independent experiments.

unlike SCNP**1** might reside extracellularly thereby allowing drug synthesis and screening without the nanoparticle potentially affecting the intracellular environment. Albertazzi and Palmans reported that catalytic Jeffamine-based SCNP could be kept largely in the extracellular space under certain conditions.[19] Therefore, the cytotoxicity and cell permeability of the SCNP were investigated. Using HeLa cells, SCNP**2** was found to exhibit significant cytotoxicity at concentrations ≥ 8 μM (Fig. S3). The uptake was assessed by labelling both SCNP**1** and SCNP**2** with Cy5 (see Supporting Information for details). HeLa cells were incubated in the DMEM media (10% FBS added) containing 2 μM of Cu^{II}-SCNP**1**-Cy5 or Cu^{II}-SCNP**2**-Cy5 for 24 h. As shown in Figure 6a, the red fluorescence within the cells indicated Cu^{II}-SCNP**1**-Cy5 was taken up, whereas almost no fluorescence was found intracellularly when the HeLa cells were treated with Cu^{II}-SCNP**2**-Cy5. This observation confirms that under these conditions SCNP**2** is "nonsticky" and exhibits poor cell penetration.

To test whether the extracellular catalyst is active and can produce small molecule products that can subsequently enter the cell through passive diffusion (Figure 6b),[31] the fluorogenic click reaction between Az**1** and Al**1** was performed with HeLa cells and Cu^{I}-SCNP**2** in PBS buffer. A concentration of 500 nM was used that is below the concentration where a similar Jeffamine-based SCNP remained in the extracellular space for several hours.[19] As shown in Figure 6c, after the reaction initiation by adding NaAsc, the fluorescence intensity of the HeLa cells gradually increased and reached the maximum in about 10 min. This result suggests that although the nanoparticle cannot penetrate the cell membrane, its reaction products readily diffuse inside the cells.

Click chemistry has been successfully applied to drug screening because it can generate a large number of compounds in high yields.[32,33] Recently, by using "SuFEx" click chemistry,[34] Dong and Sharpless reported a method to convert primary amines into azido groups which could subsequently react with alkynes to generate a large library.[35] The relatively low activity of traditional copper catalysts means that the CuAAC reactions are typically performed at millimolar concentration of substrates and catalysts, thereby requiring an organic solvent to solubilize the reagents. Thus, the products are purified and subsequently transferred to cells to test their bioactivity. The bioorthogonality and high activity of the Cu^{I}-SCNP**2** clickase provides an opportunity for in situ drug synthesis, streamlining the screening. In particular, the ability to obtain near quantitative yields of click products at micromolar concentrations[20] is important because this is the effective concentration range of many anticancer agents.

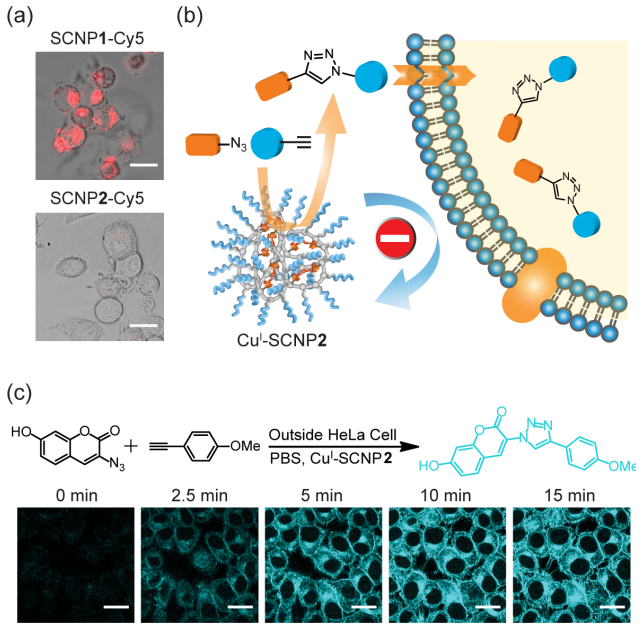

Figure 6. Cell uptake ability of SCNPs and extracellular synthesis. (a) The confocal images of HeLa cells incubated with 2 μM of Cu^{II}-SCNP**1**-Cy5 or Cu^{II}-SCNP**2**-Cy5 for 24 h in DMEM media (10% FBS added). (b) Schematic illustration of extracellular CuAAC synthesis where the nanoparticle stayed outside the cells and the reaction products defused in. (c) The confocal images over time of fluorogenic reaction outside HeLa cells performed in PBS buffer containing: [Cu^{I}-SCNP**2**] = 1 μM, [Az**1**] = 20 μM, [Al**1**] = 20 μM and [NaAsc] = 200 μM.

The proof of concept, anticancer agent screening method developed is based on the in situ, extracellular click reaction between 10 azido substrates (Az**2**-**11**) and 6 alkyne substrates (Al**1**-**6**). Screening of the 60 possible triazole products was performed by using a 96 wells plate with HeLa cells in a fast and high-throughput manner. To each well was added 50 μL of PBS buffer containing [Cu^{I}-SCNP**2**] = 1 μM, [Az] = 40 μM, [Al] = 40 μM and [NaAsc] = 100 μM, and the reaction was allowed to proceed outside the cell for 30 min, long enough for full conversion (Figure S8). To each well was added 50 μL of DMEM media (10% FBS), and the cells were incubated for 24 h. The cell viability was measured by using the MTT assay, the results presented in Figure 7. Different levels of cytotoxicity were observed for the screened compounds, the most of toxic compounds were the derivatives of triphenyl phosphonium, phenyl methoxy compound and colchicine. We chemically synthesized and purified click product Al**3**-Az**3**, and its cytotoxicity towards HeLa cells was studied more carefully. Thus, a dose-dependent cytotoxicity was observed with an IC_{50} = 24 μM, consistent with the screening result (Figure S10). The toxicity of this compound likely arises because the triphenyl phosphonium group (Al**3**)

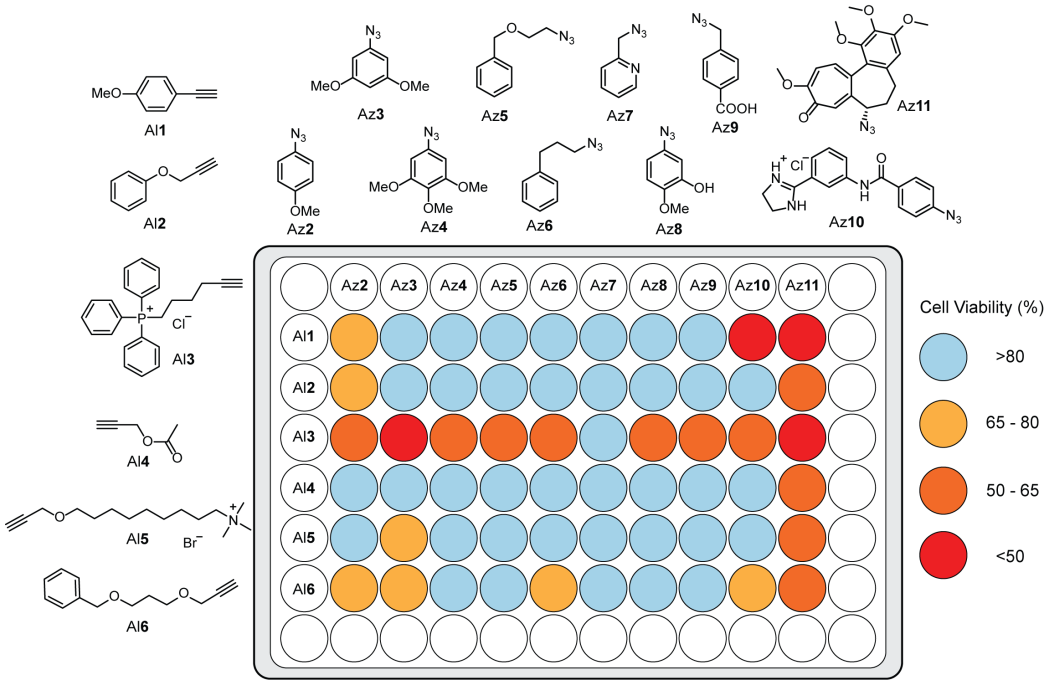

Figure 7. Cu^{I}-SCNP**2** mediated CuAAC synthesis and drug screening extracellularly. The chemical structures of the substrates and their numbering are presented. Reactions were performed outside HeLa cells in a 96 wells plate, where the PBS buffer contained: [Cu^{I}-SCNP**2**] = 1 μM, [Az] = 40 μM, [Al] = 40 μM and [NaAsc] = 100 μM. The data was presented as duplicated experiments.

brings the phenyl methoxy unit (Az**3**) into cell mitochondria and disrupts its function.[36-38]

■ CONCLUSION

We previously demonstrated the high CuAAC activity of Cu^{I}-SCNP**1** in performing the click reaction between small molecules (uptake mode). Surprisingly the utility of this catalyst extended to protein surface reactions because of the unexpected discovery of an "attach mode" wherein the SCNP binds protein surfaces using both electrostatic and hydrophobic interactions. Although this added functionality can be useful, it limits some potential applications. The Cu^{I}-SCNP**2** clickase developed here, retains the high reactivity and selectivity in performing the CuAAC (click) reaction on small molecules, but its PEGylated shell serves as a protein and cell membrane gate. Thus, the bioorthogonal click reaction is performed by a polymeric catalyst that is itself bioorthogonal. This new selectivity enables a fluorescent assay for studying protein-ligand binding, with Cu^{I}-SCNP**1** and Cu^{I}-SCNP**2** acting in combination as a dual logical gate. The PEG groups also prevent the cell uptake of the nanoparticle. As a result, Cu^{I}-SCNP**2** resides extracellularly and serves as a nanoscale factory to produce bioactive compounds in situ at the low concentrations often used in bioassays. The application to a potential anticancer agent screening method was demonstrated. More broadly, this work points to the utility of synthetic polymers as artificial enzymes with versatile, non-natural functions for bioapplications.

ASSOCIATED CONTENT

Supporting Information.
The Supporting Information is available free of charge at:

General experimental procedures and detailed synthetic procedures and characterization data for small molecules and polymers, and additional kinetic data along with details of the computational methods (PDF)

AUTHOR INFORMATION

Corresponding Author

Steven C. Zimmerman - *Department of Chemistry, Center for Biophysics and Quantitative Biology, University of Illinois, Urbana, Illinois 61801, United States;* orcid.org/0000-0002-5333-3437; E-mail: sczimmer@illinois.edu.

Authors

Junfeng Chen - *Department of Chemistry, University of Illinois, Urbana, Illinois 61801, United States*; orcid.org/0000-0002-7100-0839

Ke Li - *Department of Chemistry, University of Illinois, Urbana, Illinois 61801, United States*; orcid.org/0000-0003-3851-7710

Sarah E. Bonson - *Department of Chemistry, University of Illinois, Urbana, Illinois 61801, United States*; orcid.org/0000-0003-4167-3730

Complete contact information is available at:
https://

Notes
The authors declare no competing financial interest.

ACKNOWLEDGMENT

This work was supported by the National Science Foundation (NSF CHE-1709718, NSF GRFP DGE-1746047) and the National Institutes of Health (R01 AR069645).

REFERENCES

(1) Tonga, G. Y.; Jeong, Y.; Duncan, B.; Mizuhara, T.; Mout, R.; Das, R.; Kim, S. T.; Yeh, Y.-C.; Yan, B.; Hou, S.; Rotello, V. M., Supramolecular regulation of bioorthogonal catalysis in cells using nanoparticle-embedded transition metal catalysts. *Nat. Chem.* **2015,** *7*, 597-603.

(2) Brevé, T. G.; Filius, M.; Araman, C.; van der Helm, M. P.; Hagedoorn, P.-L.; Joo, C.; van Kasteren, S. I.; Eelkema, R., Conditional Copper-Catalyzed Azide–Alkyne Cycloaddition by Catalyst Encapsulation. *Angew. Chem. Int. Ed.* **2020,** *59*, 9340-9344.

(3) Kaphan, D. M.; Levin, M. D.; Bergman, R. G.; Raymond, K. N.; Toste, F. D., A supramolecular microenvironment strategy for transition metal catalysis. *Science* **2015,** *350*, 1235-1238.

(4) Yang, Q.; Xu, Q.; Jiang, H.-L., Metal–organic frameworks meet metal nanoparticles: synergistic effect for enhanced catalysis. *Chem. Soc. Rev.* **2017,** *46*, 4774-4808.

(5) Blackman, L. D.; Varlas, S.; Arno, M. C.; Houston, Z. H.; Fletcher, N. L.; Thurecht, K. J.; Hasan, M.; Gibson, M. I.; O'Reilly, R. K., Confinement of Therapeutic Enzymes in Selectively Permeable Polymer Vesicles by Polymerization-Induced Self-Assembly (PISA) Reduces Antibody Binding and Proteolytic Susceptibility. *ACS Cent. Sci.* **2018,** *4*, 718-723.

(6) Rubio-Cervilla, J.; González, E.; Pomposo, J., Advances in Single-Chain Nanoparticles for Catalysis Applications. *Nanomaterials* **2017,** *7*, 341-360.

(7) Mavila, S.; Eivgi, O.; Berkovich, I.; Lemcoff, N. G., Intramolecular Cross-Linking Methodologies for the Synthesis of Polymer Nanoparticles. *Chem. Rev.* **2016,** *116*, 878-961.

(8) Ouchi, M.; Badi, N.; Lutz, J.-F.; Sawamoto, M., Single-chain technology using discrete synthetic macromolecules. *Nat. Chem.* **2011,** *3*, 917-924.

(9) Huurne, G. M. t.; Palmans, A. R. A.; Meijer, E. W., Supramolecular Single-Chain Polymeric Nanoparticles. *CCS Chemistry* **2019,** *1*, 64-82.

(10) Chen, J.; Garcia, E. S.; Zimmerman, S. C., Intramolecularly Cross-Linked Polymers: From Structure to Function with Applications as Artificial Antibodies and Artificial Enzymes. *Acc. Chem. Res.* **2020**.

(11) Cole, J. P.; Hanlon, A. M.; Rodriguez, K. J.; Berda, E. B., Protein-like structure and activity in synthetic polymers. *J. Polym. Sci., Part A: Polym. Chem.* **2017,** *55*, 191-206.

(12) Pomposo, J. A., Ed. *Single-Chain Polymer Nanoparticles: Synthesis, Characterization, Simulations, and Applications*; John Wiley & Sons, **2017**.

(13) Terashima, T.; Mes, T.; De Greef, T. F. A.; Gillissen, M. A. J.; Besenius, P.; Palmans, A. R. A.; Meijer, E. W., Single-Chain Folding of Polymers for Catalytic Systems in Water. *J. Am. Chem. Soc.* **2011,** *133*, 4742-4745.

(14) Liu, Y.; Pauloehrl, T.; Presolski, S. I.; Albertazzi, L.; Palmans, A. R. A.; Meijer, E. W., Modular Synthetic Platform for the Construction of Functional Single-Chain Polymeric Nanoparticles: From Aqueous Catalysis to Photosensitization. *J. Am. Chem. Soc.* **2015,** *137*, 13096-13105.

(15) Huerta, E.; Stals, P. J. M.; Meijer, E. W.; Palmans, A. R. A., Consequences of Folding a Water-Soluble Polymer Around an Organocatalyst. *Angew. Chem.* **2013,** *125*, 2978-2982.

(16) Chen, J.; Wang, J.; Bai, Y.; Li, K.; Garcia, E. S.; Ferguson, A. L.; Zimmerman, S. C., Enzyme-like Click Catalysis by a Copper-Containing Single-Chain Nanoparticle. *J. Am. Chem. Soc.* **2018,** *140*, 13695-13702.

(17) Bai, Y.; Feng, X.; Xing, H.; Xu, Y.; Kim, B. K.; Baig, N.; Zhou, T.; Gewirth, A. A.; Lu, Y.; Oldfield, E.; Zimmerman, S. C., A Highly Efficient Single-Chain Metal–Organic Nanoparticle Catalyst for Alkyne–Azide "Click" Reactions in Water and in Cells. *J. Am. Chem. Soc.* **2016,** *138*, 11077-11080.

(18) Chen, J.; Li, K.; Shon, J. S. L.; Zimmerman, S. C., Single-Chain Nanoparticle Delivers a Partner Enzyme for Concurrent and Tandem Catalysis in Cells. *J. Am. Chem. Soc.* **2020,** 142, 4565-4569.

(19) Liu, Y.; Pujals, S.; Stals, P. J. M.; Paulöhrl, T.; Presolski, S. I.; Meijer, E. W.; Albertazzi, L.; Palmans, A. R. A., Catalytically Active Single-Chain Polymeric Nanoparticles: Exploring Their Functions in Complex Biological Media. *J. Am. Chem. Soc.* **2018,** *140*, 3423-3433.

(20) Chen, J.; Wang, J.; Li, K.; Wang, Y.; Gruebele, M.; Ferguson, A. L.; Zimmerman, S. C., Polymeric "Clickase" Accelerates the Copper Click Reaction of Small Molecules, Proteins, and Cells. *J. Am. Chem. Soc.* **2019,** *141*, 9693-9700.

(21) Kolb, H. C.; Finn, M. G.; Sharpless, K. B., Click Chemistry: Diverse Chemical Function from a Few Good Reactions. *Angew. Chem. Int. Ed.* **2001,** *40*, 2004-2021.

(22) Blümmel, J.; Perschmann, N.; Aydin, D.; Drinjakovic, J.; Surrey, T.; Lopez-Garcia, M.; Kessler, H.; Spatz, J. P., Protein repellent properties of covalently attached PEG coatings on nanostructured SiO2-based interfaces. *Biomaterials* **2007,** *28*, 4739-4747.

(23) Besanceney-Webler, C.; Jiang, H.; Zheng, T.; Feng, L.; Soriano del Amo, D.; Wang, W.; Klivansky, L. M.; Marlow, F. L.; Liu, Y.; Wu, P., Increasing the Efficacy of Bioorthogonal Click Reactions for Bioconjugation: A Comparative Study. *Angew. Chem. Int. Ed.* **2011,** *50*, 8051-8056.

(24) Mayer, M.; Meyer, B., Characterization of Ligand Binding by Saturation Transfer Difference NMR Spectroscopy. *Angew. Chem. Int. Ed.* **1999,** *38*, 1784-1788.

(25) Vasile, F.; Menchi, G.; Lenci, E.; Guarna, A.; Potenza, D.; Trabocchi, A., Insight to the binding mode of triazole RGD-peptidomimetics to integrin-rich cancer cells by NMR and molecular modeling. *Biorg. Med. Chem.* **2016,** *24*, 989-994.

(26) Neffe, A. T.; Bilang, M.; Meyer, B., Synthesis and optimization of peptidomimetics as HIV entry inhibitors against the receptor protein CD4 using STD NMR and ligand docking. *Org. Biomol. Chem.* **2006,** *4*, 3259-3267.

(27) Sivakumar, K.; Xie, F.; Cash, B. M.; Long, S.; Barnhill, H. N.; Wang, Q., A Fluorogenic 1,3-Dipolar Cycloaddition Reaction of 3-Azidocoumarins and Acetylenes. *Org. Lett.* **2004,** *6*, 4603-4606.

(28) Supuran, C. T., Carbonic anhydrases: novel therapeutic applications for inhibitors and activators. *Nat. Rev. Drug Discov.* **2008,** *7*, 168-181.

(29) Sakamoto, K. M.; Kim, K. B.; Kumagai, A.; Mercurio, F.; Crews, C. M.; Deshaies, R. J., Protacs: Chimeric molecules that target proteins to the Skp1–Cullin–F box complex for ubiquitination and degradation. *Proc. Natl. Acad. Sci.* **2001,** *98*, 8554-8559.

(30) An, S.; Fu, L., Small-molecule PROTACs: An emerging and promising approach for the development of targeted therapy drugs. *EBioMedicine* **2018,** *36*, 553-562.

(31) Clavadetscher, J.; Hoffmann, S.; Lilienkampf, A.; Mackay, L.; Yusop, R. M.; Rider, S. A.; Mullins, J. J.; Bradley, M., Copper Catalysis in Living Systems and In Situ Drug Synthesis. *Angew. Chem. Int. Ed.* **2016,** *55*, 15662-15666.

(32) Kolb, H. C.; Sharpless, K. B., The growing impact of click chemistry on drug discovery. *Drug Discov. Today* **2003,** *8*, 1128-1137.

(33) Thirumurugan, P.; Matosiuk, D.; Jozwiak, K., Click Chemistry for Drug Development and Diverse Chemical–Biology Applications. *Chem. Rev.* **2013,** *113*, 4905-4979.

(34) Dong, J.; Krasnova, L.; Finn, M. G.; Sharpless, K. B., Sulfur(VI) Fluoride Exchange (SuFEx): Another Good Reaction for Click Chemistry. *Angew. Chem. Int. Ed.* **2014,** *53*, 9430-9448.

(35) Meng, G.; Guo, T.; Ma, T.; Zhang, J.; Shen, Y.; Sharpless, K. B.; Dong, J., Modular click chemistry libraries for functional screens using a diazotizing reagent. *Nature* **2019,** *574*, 86-89.

(36) Sabharwal, S. S.; Schumacker, P. T., Mitochondrial ROS in cancer: initiators, amplifiers or an Achilles' heel? *Nat. Rev. Cancer* **2014,** *14*, 709-721.

(37) Pagliai, F.; Pirali, T.; Del Grosso, E.; Di Brisco, R.; Tron, G. C.; Sorba, G.; Genazzani, A. A., Rapid Synthesis of Triazole-Modified Resveratrol Analogues via Click Chemistry. *J. Med. Chem.* **2006,** *49*, 467-470.

(38) Wang, F.; Zhang, Y.; Liu, Z.; Du, Z.; Zhang, L.; Ren, J.; Qu, X., A Biocompatible Heterogeneous MOF–Cu Catalyst for In Vivo Drug Synthesis in Targeted Subcellular Organelles. *Angew. Chem. Int. Ed.* **2019,** *58*, 6987-6992.

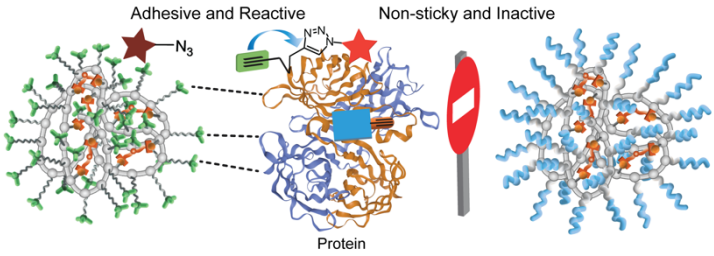
Adhesive and Reactive
Non-sticky and Inactive
N_3
Protein